NIH Public Access
Author Manuscript
Science. Author manuscript; available in PMC 2014 December 20.

Published in final edited form as:
Science. 2013 December 20; 342(6165): 1484–1490. doi:10.1126/science.1245627.

Cryo-EM structure of a fully glycosylated soluble cleaved HIV-1 Env trimer

Dmitry Lyumkis[1,2], **Jean-Philippe Julien**[2,3,4], **Natalia de Val**[2,3], **Albert Cupo**[6], **Clinton S. Potter**[1,2], **Per Johan Klasse**[6], **Dennis R. Burton**[3,5,7,8], **Rogier W. Sanders**[6,9], **John P. Moore**[6], **Bridget Carragher**[1,2,†], **Ian A. Wilson**[2,3,4,5,†], and **Andrew B. Ward**[2,3,5,†]

[1]National Resource for Automated Molecular Microscopy, The Scripps Research Institute, La Jolla, California, 92037, USA [2]Department of Integrative Structural and Computational Biology, The Scripps Research Institute, La Jolla, California 92037, USA [3]Center for HIV/AIDS Vaccine Immunology and Immunogen Discovery, The Scripps Research Institute, La Jolla, California 92037, USA [4]Skaggs Institute for Chemical Biology, The Scripps Research Institute, La Jolla, California 92037, USA [5]IAVI Neutralizing Antibody Center, The Scripps Research Institute, La Jolla, California 92037, USA [6]Weill Medical College of Cornell University, New York, New York 10021, USA [7]Department of Immunology and Microbial Science, The Scripps Research Institute, La Jolla, California 92037, USA [8]Ragon Institute of MGH, MIT, and Harvard, Cambridge, MA 02129, USA [9]Department of Medical Microbiology, Academic Medical Center, Amsterdam, Netherlands

Abstract

The HIV-1 envelope glycoprotein (Env) trimer contains the receptor binding sites and membrane fusion machinery that introduce the viral genome into the host cell. As the only target for broadly neutralizing antibodies (bnAbs), Env is a focus for rational vaccine design. We present a cryo-electron microscopy reconstruction and structural model of a cleaved, soluble SOSIP gp140 trimer in complex with a CD4 binding site (CD4bs) bnAb, PGV04, at 5.8 Å resolution. The structure reveals the spatial arrangement of Env components, including the V1/V2, V3, HR1 and HR2 domains, and shielding glycans. The structure also provides insights into trimer assembly, gp120-gp41 interactions, and the CD4bs epitope cluster for bnAbs, which covers a more extensive area and defines a more complex site of vulnerability than previously described.

HIV-1 currently infects over 34 million people worldwide and causes AIDS. The availability of antiviral therapies has greatly reduced the death toll, particularly in the Western world, but has not yet reduced the global spread of this deadly pathogen. A successful preventative vaccine would be a significant step towards this critical goal. The trimeric viral envelope glycoprotein (Env) spike, a major vaccine development target (1), consists of three gp120 subunits that contain the CD4 receptor and co-receptor binding sites and three gp41 subunits that drive membrane fusion. Immune selection pressure creates extensive Env sequence variation that complicates vaccine development, but trimer-targeting broadly neutralizing antibodies (bnAbs) provide important clues about vulnerable Env sites (1). Critical features of bnAb epitopes have been revealed by x-ray structures of Fab complexes with the gp120 core, gp120 outer domain, gp41 peptides, scaffolded epitopes, or glycan arrays (2–9). These structures are based on only a subcomponent of the Env spike and do not reveal the full complement of inter-subunit contacts and constraints. Low-resolution electron microscopy

[†]To whom correspondence should be addressed: abward@scripps.edu (A.B.W.), bcarr@scripps.edu (B.C.), wilson@scripps.edu (I.A.W.).

NIH-PA Author Manuscript
NIH-PA Author Manuscript
NIH-PA Author Manuscript

NIH-PA Author Manuscript

NIH-PA Author Manuscript

NIH-PA Author Manuscript

(EM) structures of the trimer provide an overall architecture (10–16), but do not define the molecular details of bnAb epitopes. Here we have used cryo-EM to study soluble, cleaved recombinant trimers stabilized by specific substitutions (17, 18). These BG505 SOSIP.664 gp140 trimers are highly stable and homogeneous, have a near native antigenicity profile (19) and a well-defined shape when viewed by negative stain EM at intermediate resolution (11, 12, 14, 20). We now present the cryo-EM structure at 5.8 Å resolution of this Env trimer in complex with bnAb PGV04 against a CD4bs epitope. The structure reveals the overall organization of Env, the interaction between gp120 and gp41 subunits, and how trimer formation affects the CD4bs and its associated bnAb epitopes.

Specimen preparation, EM data acquisition, and image processing of SOSIP trimers

BG505 SOSIP.664 gp140 trimers were produced in HEK 293T cells and, hence, have a typical human cell glycosylation profile. The Env trimer is relatively small by EM standards (~425 kDa, of which almost half is glycan) and lacks features that facilitate high-resolution image processing (21). We therefore adopted a recently described cryo-EM feature-enhancement strategy (22), by adding PGV04 Fabs as fiducial markers for computational alignment of the trimer. We recorded the EM data on a direct electron detector, which improves the signal compared to conventional methods and enables correction for beam-induced motion and specimen drift (23). New image processing algorithms, similar to those that have recently provided near-atomic resolution characterization of select macromolecular complexes (24, 25), were used in the analysis. Together, these cryo-EM technical advances, combined with design and production of a stable soluble Env trimer, have enabled the reconstruction of the SOSIP.664:PGV04 complex to 5.8 Å resolution (Fig. 1 and fig. S1). The reconstructed electron potential map provided sufficient detail for modeling most of gp120, including the variable loops and the heptad repeat 1 (HR1) and HR2 components of gp41 (Fig. 1 and fig. S1). The EM reconstruction was validated by the appearance of the Fab and gp120 densities that were in excellent agreement with the previously determined structures, by several recently described quantitative metrics for EM (fig. S2) (21, 26, 27) and also by an independently obtained X-ray structure of the same trimer (but from HEK 293S GnT−/− cells and hence with a simpler glycan profile) in complex with the PGT122 bnAb at a similar resolution (28). The EM map presented here is significantly improved in resolution and in new features compared to previous trimer reconstructions; it also revealed additional density that is consistent with N-linked glycans on both gp120 and gp41 (fig. S4) (29).

Structural arrangement of gp120 and variable loops V1, V2, and V3

The gp120 core crystal structure in complex with PGV04 (PDB 3SE9, (30)) was docked into the EM map and further refined (see supplementary online material (31)). The crystal structure of a scaffolded V1/V2 protein (PDB 3U2S (9)) could also be fitted into density at the trimer apex without significant rearrangements (Fig. 2A and fig. S5A). Densities corresponding to GlcNAc residues of the glycans at the N156 and N160 sites (HXB2 numbering) within V1/V2 are apparent at the trimer apex (Fig. 2C and figs. S4 and S5A), and are consistent with the arrangement of the V1/V2 N156 and N160 glycans predicted by a low-resolution model of the same trimers in complex with bnAb PG9 (14). The V1 loop is in a slightly different conformation than in scaffolded ZM109 V1/V2 (9). The V2 loop could not be built in its entirety but was localized above the CD4 binding site (fig. S5A–B) in a position to restrict access to the CD4bs (discussed below). The V3 loop is situated directly beneath the V1/V2 hairpin with the tip pointing toward the trimer axis and interacting with the V2 base from the adjacent protomer, in a different configuration than previously observed (Fig. 2B and figs. S5A and C). The N197 glycan at the V2 base sits at the inter-

NIH-PA Author Manuscript

NIH-PA Author Manuscript

NIH-PA Author Manuscript

protomer interface (Fig. 2C and fig. S5A) and may shield V3 epitopes on the trimer; various V3 antibodies have higher affinities for monomeric than trimeric Env, implicating the existence of such steric constraints (32, 33). Overall, the gp120 subunits have a compact globular configuration and are assembled into a trimer via a limited set of interactions at the apex that involve the V1/V2 and V3 loop structures (Figs. 1 and 2C). This arrangement exposes several basic residues at the trimer apex that are important targets for bnAbs such as PG9, PG16, PGT145 and CH01, which have acquired negatively charged sulfated tyrosine moieties in their paratopes (9) (Fig. 2D).

Structural arrangement of gp41

Gp41 forms a pedestal at the base of the trimer (Fig. 3, A and B). Each protomer is characterized by two long, prominent helices. The first (HR1) forms a three-helix bundle with the neighboring protomers in the trimer core; the second (HR2) wraps around the outer periphery of the trimer base, angling downward and with its C-terminus proximal to the viral membrane (Fig. 3, A and B). The three-helix bundle is formed by the C-terminal half of HR1 and resembles the arrangement in the crystal structure of post-fusion gp41 (34), and also in the proposed open, intermediate state seen by single-particle EM (35) (Fig. 3, C and D). To assess whether the three-helix bundle is a feature induced by PGV04 binding, we calculated an independent, 12.7 Å reconstruction of the unliganded trimer (fig. S6). The three-helix bundle was present in this unliganded structure; hence, it is likely that the gp41 conformation that we describe here represents the ground state, and not an activated intermediate, as previously suggested (35). Just above the three-helix bundle and below the trimer apex, we observe a small opening that is continuous with the exterior (fig. S7). The large hole that is a previously reported feature of the trimer core is likely a result of lower resolution reconstructions (> 20 Å) (36), as illustrated in fig. S3A.

To identify the gp41 C-terminus, we calculated an ~8 Å reconstruction of a similar trimer but with the last 14 amino acids deleted (designated SOSIP.650) (Fig. 3E). Difference maps showed that a segment corresponding to ~3.5 helical turns, or ~14 amino acids, was absent from the SOSIP.650 reconstruction (Fig. 3E and fig. S8). Additionally, our data indicate that residues around 650 in HR2 interact strongly with the bottom of HR1 (fig. S9) (37).

The N-terminal half of HR1, including a short helix, and the fusion peptide proximal region (FPPR) and fusion peptide (FP) emanate from the top of the internal coiled coil around the three-fold axis and turn down toward the trimer base (Fig. 3A). The internal region at the base of the trimer contains additional density that could not be assigned unambiguously, but likely corresponds to the intervening residues between HR1 and HR2, as well as the gp120 C1 and C5 regions (Fig. 3, A and B). This interpretation is consistent with the known inter-subunit interactions between gp120 C1/C5 and gp41 residues ~589–610 (18). This element of gp41 contains the internal disulfide bonded loop and also the engineered Cys substitutions that covalently link gp120 residue-501 to gp41 residue-605 via a disulfide bond in SOSIP gp140s (18). The relatively hydrophobic gp120 N- and C-termini and nearby gp41 residues are all sequestered towards the middle of the trimer. We have putatively assigned the hydrophobic FP to this solvent-inaccessible region (Fig. 3B); there are similarities here to influenza hemagglutinin, another type I fusion protein (28, 38). Localization at the gp120/gp41 interface would allow the FP to be released in response to CD4 and co-receptor-induced conformational changes within gp120 and gp41 that drive membrane fusion.

PGV04 binding site on the Env trimer

Subtle differences in the Fab PGV04 interaction with gp120 are apparent when the monomeric and trimeric forms of core gp120 are aligned, which may be explained by trimer-specific contacts (Fig. 4A). On the glycosylated trimer, the Fab light chain interacts

NIH-PA Author Manuscript

NIH-PA Author Manuscript

NIH-PA Author Manuscript

extensively with glycan N276 (Fig. 4B and fig. S17). The same glycan prevents the VRC01 germline antibody from binding to gp120 monomers (39), so it may be a general impediment to this bNAb class. The glycosylated trimer EM structure also contains additional density for a region corresponding to the V2 loop and/or glycans (Fig. 4B) that likely play a role in recognition of the CD4bs.

Many SOSIP.664 trimer particles had <3 PGV04 Fabs bound, despite the Fab being in molar excess of trimer during sample preparation. We used template-based 3D sorting of single particle images to generate trimer populations with 3, 2, 1 and 0 Fabs bound. Each of the subsets was then independently refined to generate maps with resolutions of 5.8 Å, 7.9 Å, 16.9 Å and 19.1 Å, respectively (figs. S10–S15). The 7.9 Å, 2-Fab reconstruction (Fig. 4C) was sufficient to interpret subtle structural differences created by the presence or absence of a bound Fab. Specifically, PGV04 binding induced positive density corresponding to the putative V2 loop and/or glycans N363/386 (Fig. 4D). Additional density corresponding to glycan N301 from the neighboring gp120 protomer and N276 from the same gp120 protomer was also seen to interact with PGV04 (fig. S16C) (40). One interpretation is that PGV04 binding stabilizes both the glycans and the flexible loops in the trimer structure.

Solution isothermal titration calorimetry (ITC) measurements also revealed that PGV04 bound BG505 SOSIP.664 trimers in a sub-stoichiometric manner (<2), consistent with the EM results (Fig. 4E). The EM map does not reveal an obvious structural impediment to stoichiometric PGV04 binding (i.e., 3 per trimer). One hypothesis for why some trimers do not bind the bnAb or do so at a low stoichiometry is that incomplete or differential glycan processing creates some micro-heterogeneity. When we measured PGV04 binding to 293S cell-produced trimers that bear only high mannose sugars, it was again sub-stoichiometric (i.e., <2). However, when the latter trimers were enzymatically deglycosylated, the number of bound Fabs increased from <2 to ~2.5 and the average Kd improved to 73nM from 135nM; the implication is that specific glycans of variable composition and size can indeed interfere with antibody binding to the CD4bs. The unfavorable entropic contribution of the binding signal was also significantly lower for the deglycosylated trimers (Fig. 4F). The entropic cost of locking normally flexible glycans in place may be yet another viral defense against antibodies, potentially one that restricts the stimulation of bnAb germline B-cell receptors (39, 41). Eliminating such glycans may help the design of immunogens intended to induce CD4bs antibodies (39, 41).

Quaternary nature of the CD4 binding site

The CD4bs is relatively highly conserved and immunogenic in the context of HIV-1 infection. Env subunit vaccines, such as monomeric gp120 and uncleaved gp140s, have failed to elicit bnAbs against this site, while often inducing non- or poorly-neutralizing Abs that recognize overlapping epitopes (1). One implication is that the structure and immunogenicity of the CD4bs are adversely affected when presented in a non-native context; thus, if the site assumes the CD4-bound state (42), the outcome may be the predominant elicitation of antibodies that are non-neutralizing because they cannot bind to native trimers. The EM structure that we describe delineates the narrow range of approach angles available to CD4bs bnAbs when engaging the trimer, and shows how epitope complexity makes it difficult to target this site effectively via non-native immunogens. Amongst new information are the following points:

The CD4-induced subdomain known as the bridging sheet is presented on the SOSIP.664 gp140 trimers differently from how it appears on various versions of monomeric gp120 (42). Specifically, the strand arrangement at the base of V1/V2 is reversed on the trimer, such that V2 forms an adjacent/parallel interaction with β-20 instead of the anti-parallel β -interaction

NIH-PA Author Manuscript

NIH-PA Author Manuscript

NIH-PA Author Manuscript

between the V1 base and β-20 found in the gp120 core (Fig. 5A and fig. S18). Thus, quaternary interactions mean that the topological relationship between the base of V2, which includes the N197 glycan, and the CD4bs is not the same on trimeric and monomeric gp120.

The neighboring protomer also plays a significant role in restricting access to the CD4bs. When the heavy chain of PGV04 or the related VRC01 bnAb binds the trimer, it is within 5 Å of a loop (residues 61–62) that precedes a short α-helix (α-0) in C1 of a neighboring gp120 protomer (Fig. 5B); likewise, when CD4 (PDB 4JM2) is docked into the CD4bs on the trimer, it also contacts an adjacent protomer (Fig. 5B). The α-0 helix is directly downstream from His66, a residue implicated in regulating the sampling of the CD4-bound conformation (43). Thus, the first stage of CD4 binding may require the trimer to flex to an extent, but once initial contact is made, the trimer is further destabilized, and co-receptor binding and fusion can proceed.

Docking CD4bs antibodies with a range of neutralization capabilities into the EM trimer model suggests that the crystal structures of monomeric gp120-Ab complexes do not completely define this epitope cluster. Additional, quaternary structure-dependent contacts are important for CD4bs Fabs to recognize trimeric Env, with the V1/V2 loop structure influencing how they bind and, hence, neutralize (Fig. 5C). Previous mutagenesis data are now more readily interpretable; for example, we can now explain why the light chain CDR1 and CDR3 residues are essential for neutralization by the b12 bnAb (44); the trimer structure shows they are positioned to interact with V1/V2 (fig. S19). The non-neutralizing Fabs b13 (3IDX) and F105 (3HI1) (6) clash with V1/V2 (same protomer) and V3 (adjacent protomer), impeding their ability to bind the trimer (Fig 5C). These results are consistent with both BG505 virus neutralization and antibody-binding studies using the corresponding SOSIP. 664 gp140 trimers (19).

Immunoglobulin framework insertions and mutations are important for broad and potent neutralization (5). Our structure shows that framework region 3 in the heavy chain (HFR3) of CD4bs antibodies 3BNC117 (also 3BNC60), VRC03 and VRC06 interact with basic residues on an adjacent protomer (Fig 5, D and E). HFR3 insertions contain acidic residues that point toward conserved basic residues near the V3 tip of the adjacent gp120 protomer (Fig. 5E). A properly folded trimer positions these basic residues in an appropriate quaternary orientation for interacting with CD4bs bnAbs. The preference of VRC06 for cleaved over uncleaved trimers (45) is also consistent with previous observations that cleavage is critical for Env to adopt a native-like conformation (20).

Affinity maturation events in the evolution of the CH103 CD4bs bNAb involve the early appearance of acidic residues in the HFR3 loop that then persist (46). However, HFR3 makes no contact with gp120 in the crystal structure of the monomeric gp120-CH103 complex (PDB 4JAN) (46). The trimer structure now shows that HFR3 of CH103 is in close proximity to the basic residues on V3 from the adjacent gp120 (Fig. 5E). Thus, the quaternary context of the CH103 epitope helps explain why somatic hypermutation within HFR3 is critical, and why the acidic residues are conserved once they appear.

The features of the CD4bs outlined above are likely to be relevant to other bnAbs that are yet to be identified. Thus, the V3 interactions and the evolution of framework mutations essential for neutralization breadth and potency should now be taken into consideration. The quaternary constraints on these epitopes will affect how potent CD4bs bnAbs, such as VRC01, are induced and then undergo the affinity maturation process.

NIH-PA Author Manuscript

NIH-PA Author Manuscript

NIH-PA Author Manuscript

Summary

The 5.8 Å resolution cryo-EM structure presented here is very similar to the x-ray structure of the same SOSIP.664 gp140 trimers in complex with bnAb PGT122 (28). Both structures are, however, very different from a 6 Å structure recently reported for a detergent-solubilized, full-length but uncleaved trimer (47). Differences in the design of the Env trimers might contribute to some of these structural inconsistencies. Alternatively, the cryo-EM methodology used to derive the full-length, uncleaved trimer structure has been criticized and the controversy is as yet unresolved (48). Considered in isolation, our soluble SOSIP.664 gp140 trimer structures are highly consistent with known Env structure-function relationships, while revealing new information on the pre-fusion form of the trimer. The structures explain how bnAbs recognize their epitopes and why quaternary constraints prevent some non-nAbs from binding the trimer. Overall, the new information is a step towards understanding trimeric Env at atomic-level resolution. The trimer structure should also guide improvements to Env-based vaccines.

Supplementary Material

Refer to Web version on PubMed Central for supplementary material.

Acknowledgments

We thank Yifan Cheng and Xueming Li for providing raw frame alignment scripts prior to publication, to Richard Henderson for making the makestack_HRnoise. exe program available for use to assess the overfitting of the EM data, to Jacob Korzun for technical assistance, Jean-Cristophe Ducom (TSRI) for support with computational resources, and C. Richter King and W. Koff for support and encouragement. This work was supported by NIH grants HIVRAD P01 AI82362 (J.P.M., I.A.W., and A.B.W) and R01 AI36082 (I.A.W.), the International AIDS Vaccine Initiative Neutralizing Antibody Consortium (D.R.B., J.P.M., I.A.W., A.B.W.), and Center, Scripps CHAVI-ID (UM1 AI100663) (D.R.B., I.A.W., A.B.W.), a Vidi grant from the Netherlands Organization for Scientific Research (R.W.S.), a Starting Investigator Grant from the European Research Council (R.W.S.) and a Canadian Institutes of Health Research fellowship (J.-P.J.). The EM work was conducted at the National Resource for Automated Molecular Microscopy at The Scripps Research Institute, which is supported by the U. S. NIH NIGMS Biomedical Technology Research Center program (GM103310) (B.C., C.S.P.). 3D visualizations were generated using the UCSF Chimera package. The EM reconstructions will be deposited in the Electron Microscopy Data Bank under accession code *** prior to publication. The structure coordinates will be deposited in the Protein Data Bank under accession code *** prior to publication. Sharing of other materials will be subject to standard material transfer agreements. Raw EM data will be provided upon request. The content is the responsibility of the authors and does not necessarily reflect the official views of the NIGMS, NCI or NIH. The International AIDS Vaccine Initiative (IAVI) has previously filed a patent relating to the BG505 SOSIP.664 trimer: U.S. Prov. Appln. No. 61/772,739, titled “HIV-1 envelope glycoprotein”, with inventors M. Caulfield, A.C., H. Dean, S. Hoffenberg, C.R.K., P.J.K., A. Marozsan, J.P.M., R.S., A.B.W., I.A.W., J.-P.J. This is manuscript 25060 from The Scripps Research Institute.

References and Notes

1. Kwong PD, Mascola JR, Nabel GJ. Broadly neutralizing antibodies and the search for an HIV-1 vaccine: the end of the beginning. Nat Rev Immunol. 2013; 13:693. [PubMed: 23969737]
2. Kwong PD, et al. Structure of an HIV gp120 envelope glycoprotein in complex with the CD4 receptor and a neutralizing human antibody. Nature. 1998; 393:648. [PubMed: 9641677]
3. Joyce MG, et al. Outer domain of HIV-1 gp120: antigenic optimization, structural malleability, and crystal structure with antibody VRC-PG04. J Virol. 2013; 87:2294. [PubMed: 23236069]
4. Kwon YD, et al. Unliganded HIV-1 gp120 core structures assume the CD4-bound conformation with regulation by quaternary interactions and variable loops. Proc Natl Acad Sci USA. 2012; 109:5663. [PubMed: 22451932]
5. Klein F, et al. Somatic mutations of the immunoglobulin framework are generally required for broad and potent HIV-1 neutralization. Cell. 2013; 153:126. [PubMed: 23540694]

NIH-PA Author Manuscript

NIH-PA Author Manuscript

NIH-PA Author Manuscript

6. Chen L, et al. Structural basis of immune evasion at the site of CD4 attachment on HIV-1 gp120. Science. 2009; 326:1123. [PubMed: 19965434]
7. Pancera M, et al. Structure of HIV-1 gp120 with gp41-interactive region reveals layered envelope architecture and basis of conformational mobility. Proc Natl Acad Sci USA. 2010; 107:1166. [PubMed: 20080564]
8. Huang CC, et al. Structure of a V3-containing HIV-1 gp120 core. Science. 2005; 310:1025. [PubMed: 16284180]
9. McLellan JS, et al. Structure of HIV-1 gp120 V1/V2 domain with broadly neutralizing antibody PG9. Nature. 2011; 480:336. [PubMed: 22113616]
10. Khayat R, et al. Structural characterization of cleaved, soluble HIV-1 envelope glycoprotein trimers. J Virol. 2013; 87:9865. [PubMed: 23824817]
11. Kong L, et al. Supersite of immune vulnerability on the glycosylated face of HIV-1 envelope glycoprotein gp120. Nat Struct Mol Biol. 2013; 20:796. [PubMed: 23708606]
12. Julien JP, et al. Broadly neutralizing antibody PGT121 allosterically modulates CD4 binding via recognition of the HIV-1 gp120 V3 base and multiple surrounding glycans. PLoS Pathog. 2013; 9:e1003342. [PubMed: 23658524]
13. Merk A, Subramaniam S. HIV-1 envelope glycoprotein structure. Curr Opin Struct Biol. 2013; 23:268. [PubMed: 23602427]
14. Julien JP, et al. Asymmetric recognition of the HIV-1 trimer by broadly neutralizing antibody PG9. Proc Natl Acad Sci U S A. 2013; 110:4351. [PubMed: 23426631]
15. Pejchal R, et al. A potent and broad neutralizing antibody recognizes and penetrates the HIV glycan shield. Science. 2011; 334:1097. [PubMed: 21998254]
16. Harris A, et al. Trimeric HIV-1 glycoprotein gp140 immunogens and native HIV-1 envelope glycoproteins display the same closed and open quaternary molecular architectures. Proc Natl Acad Sci U S A. 2011; 108:11440. [PubMed: 21709254]
17. Sanders RW, et al. Stabilization of the soluble, cleaved, trimeric form of the envelope glycoprotein complex of human immunodeficiency virus type 1. J Virol. 2002; 76:8875. [PubMed: 12163607]
18. Binley JM, et al. A recombinant human immunodeficiency virus type 1 envelope glycoprotein complex stabilized by an intermolecular disulfide bond between the gp120 and gp41 subunits is an antigenic mimic of the trimeric virion-associated structure. J Virol. 2000; 74:627. [PubMed: 10623724]
19. Sanders RW, et al. A next-generation cleaved, soluble HIV-1 Env trimer, BG505 SOSIP.664 gp140, expresses multiple epitopes for broadly neutralizing but not non-neutralizing antibodies. PLoS Pathog. 2013
20. Ringe R, et al. Cleavage determines whether soluble HIV-1 envelope glycoprotein trimers adopt native-like conformations. Proc Natl Acad Sci U S A. 2013
21. Henderson R, et al. Tilt-pair analysis of images from a range of different specimens in single-particle electron cryomicroscopy. J Mol Biol. 2011; 413:1028. [PubMed: 21939668]
22. Wu S, et al. Fabs enable single particle cryoEM studies of small proteins. Structure. 2012; 20:582. [PubMed: 22483106]
23. Campbell MG, et al. Movies of ice-embedded particles enhance resolution in electron cryo-microscopy. Structure. 2012; 20:1823. [PubMed: 23022349]
24. Li X, et al. Electron counting and beam-induced motion correction enable near-atomic-resolution single-particle cryo-EM. Nature methods. 2013; 10:584. [PubMed: 23644547]
25. Zhang X, et al. Near-atomic resolution using electron cryomicroscopy and single-particle reconstruction. Proc Natl Acad Sci U S A. 2008; 105:1867. [PubMed: 18238898]
26. Rosenthal PB, Henderson R. Optimal determination of particle orientation, absolute hand, and contrast loss in single-particle electron cryomicroscopy. J Mol Biol. 2003; 333:721. [PubMed: 14568533]
27. Chen S, et al. High-resolution noise substitution to measure overfitting and validate resolution in 3D structure determination by single particle electron cryomicroscopy. Ultramicroscopy. 2013; 135C:24. [PubMed: 23872039]

NIH-PA Author Manuscript

NIH-PA Author Manuscript

NIH-PA Author Manuscript

28. Julien JP, et al. Crystal structure of a soluble cleaved HIV-1 Env trimer in complex with a glycan-dependent broadly neutralizing antibody. Science. 2013
29. Most of the predicted N-linked glycosylation sites had at least some additional density that could be attributed to them in the EM maps (fig. S4). Table S1 lists the predicted glycan position, whether density for a glycan was visible, and to what extent the glycan could be modeled, at least in part. Density corresponding to glycans was generally consistent between three independently determined maps, namely BG505 SOSIP.664 bound to 3 (5.8 Å) or 2 Fabs (7.9 Å), and BG505 SOSIP.650 bound to 3 Fabs (8.2 Å).
30. Wu X, et al. Focused evolution of HIV-1 neutralizing antibodies revealed by structures and deep sequencing. Science. 2011; 333:1593. [PubMed: 21835983]
31. Materials and methods are available as supplementary material on Science Online.
32. Wang W, et al. A systematic study of the N-glycosylation sites of HIV-1 envelope protein on infectivity and antibody-mediated neutralization. Retrovirology. 2013; 10:14. [PubMed: 23384254]
33. Li Y, et al. Removal of a single N-linked glycan in human immunodeficiency virus type 1 gp120 results in an enhanced ability to induce neutralizing antibody responses. J Virol. 2008; 82:638. [PubMed: 17959660]
34. Weissenhorn W, Dessen A, Harrison SC, Skehel JJ, Wiley DC. Atomic structure of the ectodomain from HIV-1 gp41. Nature. 1997; 387:426. [PubMed: 9163431]
35. Tran EE, et al. Structural mechanism of trimeric HIV-1 envelope glycoprotein activation. PLoS Pathog. 2012; 8:e1002797. [PubMed: 22807678]
36. Liu J, Bartesaghi A, Borgnia MJ, Sapiro G, Subramaniam S. Molecular architecture of native HIV-1 gp120 trimers. Nature. 2008; 455:109. [PubMed: 18668044]
37. We have found that the gp41 C-terminus in BG505 SOSIP gp140 trimers can be truncated to position 650, but further shortening leads to instability and hence subunit dissociation (R. Ringe, JPM and RWS unpublished results).
38. Wilson IA, Skehel JJ, Wiley DC. Structure of the haemagglutinin membrane glycoprotein of influenza virus at 3 A resolution. Nature. 1981; 289:366. [PubMed: 7464906]
39. Jardine J, et al. Rational HIV immunogen design to target specific germline B cell receptors. Science. 2013; 340:711. [PubMed: 23539181]
40. No such differences were observed in control cases between the Fab-labeled protomers within the 2-Fab reconstruction, or between any combination of protomers within an unsymmetrized 3-Fab reconstruction (fig. S16).
41. McGuire AT, et al. Engineering HIV envelope protein to activate germline B cell receptors of broadly neutralizing anti-CD4 binding site antibodies. J Exp Med. 2013; 210:655. [PubMed: 23530120]
42. Kwon YD, et al. Unliganded HIV-1 gp120 core structures assume the CD4-bound conformation with regulation by quaternary interactions and variable loops. Proc Natl Acad Sci U S A. 2012; 109:5663. [PubMed: 22451932]
43. Kassa A, et al. Transitions to and from the CD4-bound conformation are modulated by a single-residue change in the human immunodeficiency virus type 1 gp120 inner domain. J Virol. 2009; 83:8364. [PubMed: 19535453]
44. Zwick MB, et al. Molecular features of the broadly neutralizing immunoglobulin G1 b12 required for recognition of human immunodeficiency virus type 1 gp120. J Virol. 2003; 77:5863. [PubMed: 12719580]
45. Li Y, et al. HIV-1 neutralizing antibodies display dual recognition of the primary and coreceptor binding sites and preferential binding to fully cleaved envelope glycoproteins. J Virol. 2012; 86:11231. [PubMed: 22875963]
46. Liao HX, et al. Co-evolution of a broadly neutralizing HIV-1 antibody and founder virus. Nature. 2013; 496:469. [PubMed: 23552890]
47. Mao Y, et al. Molecular architecture of the uncleaved HIV-1 envelope glycoprotein trimer. Proc Natl Acad Sci U S A. 2013; 110:12438. [PubMed: 23757493]
48. Cohen J. Structural biology. Is high-tech view of HIV too good to be true? Science. 2013; 341:443. [PubMed: 23908196]

NIH-PA Author Manuscript

NIH-PA Author Manuscript

NIH-PA Author Manuscript

Summary

The cryo-EM structure of a soluble cleaved Env SOSIP gp140 trimer in complex with broadly neutralizing antibody PGV04 reveals key features that dictate how Env functions and how it interacts with the human immune system.

NIH-PA Author Manuscript
NIH-PA Author Manuscript
NIH-PA Author Manuscript

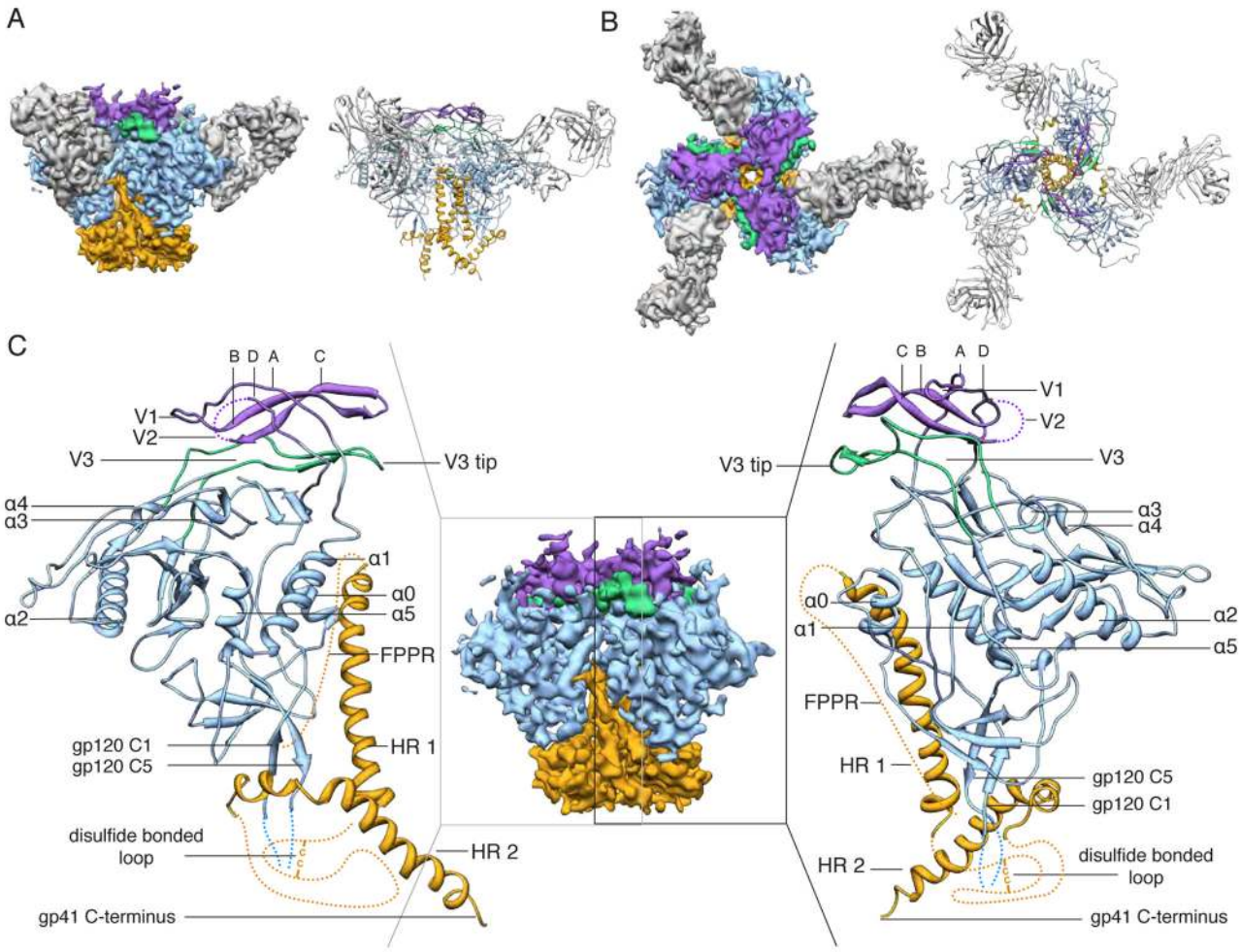

Fig. 1. 5.8 Å EM reconstruction and model of Env trimer in complex with PGV04

(**A**) Side and (**B**) top views of BG505 SOSIP trimer EM reconstruction (left) and corresponding model (right). The viral membrane would be at the bottom of the figure. Segmentation and color coding is as follows: PGV04 (gray), gp120 (blue), gp41 (orange), V1/V2 (purple), and V3 (green). (**C**) The middle panel shows a side view of the EM map alone with the Fab density removed. The outer panels show the modeled portion corresponding to the boxed region in the middle panel.

NIH-PA Author Manuscript

NIH-PA Author Manuscript

NIH-PA Author Manuscript

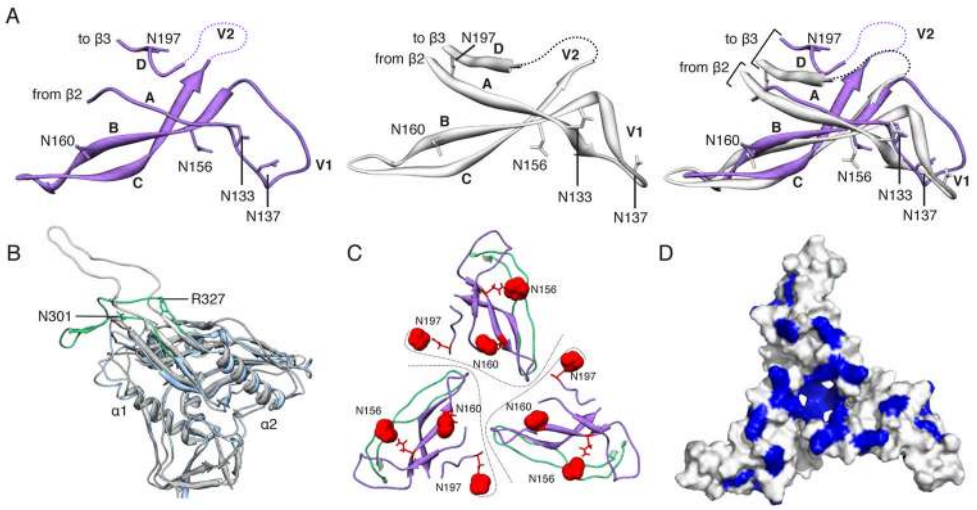

Fig. 2. Structures of gp120 V1/V2/V3 variable loops

(**A**) Comparison of the V1/V2 domain from the EM model (purple) and the previously published X-ray structure (3U2S, white) with key residues labeled. The structures are nearly identical except for the base of V1/V2 (strands A and D) and the V1 loop. (**B**) Superposition of gp120 and the V3 loop from the EM model (blue/green) onto a previous X-ray structure containing a V3 loop (2B4C, gray/white). While gp120 is structurally conserved, the V3 β-hairpin loop exhibits a different configuration. Specifically, V3 bends around a hinge formed near residues 302 and 326. The N-terminal residues of V3 up to residue 301 and the C-terminal residues after residue 327 are structurally similar. Residues 1–90, and 126–196 are omitted for clarity. (**C**) Quaternary arrangement of V1, V2, and V3 regions of gp120 at the top of the trimer. The positions of glycans at N156, N160, and N197 have been highlighted as red spheres. Lines denote approximate protomer boundaries. (**D**) Surface view of the modeled portion in **C**, with the basic residues (Arg and Lys) colored blue. A large number of basic amino acids are localized to the trimer apex.

NIH-PA Author Manuscript

NIH-PA Author Manuscript

NIH-PA Author Manuscript

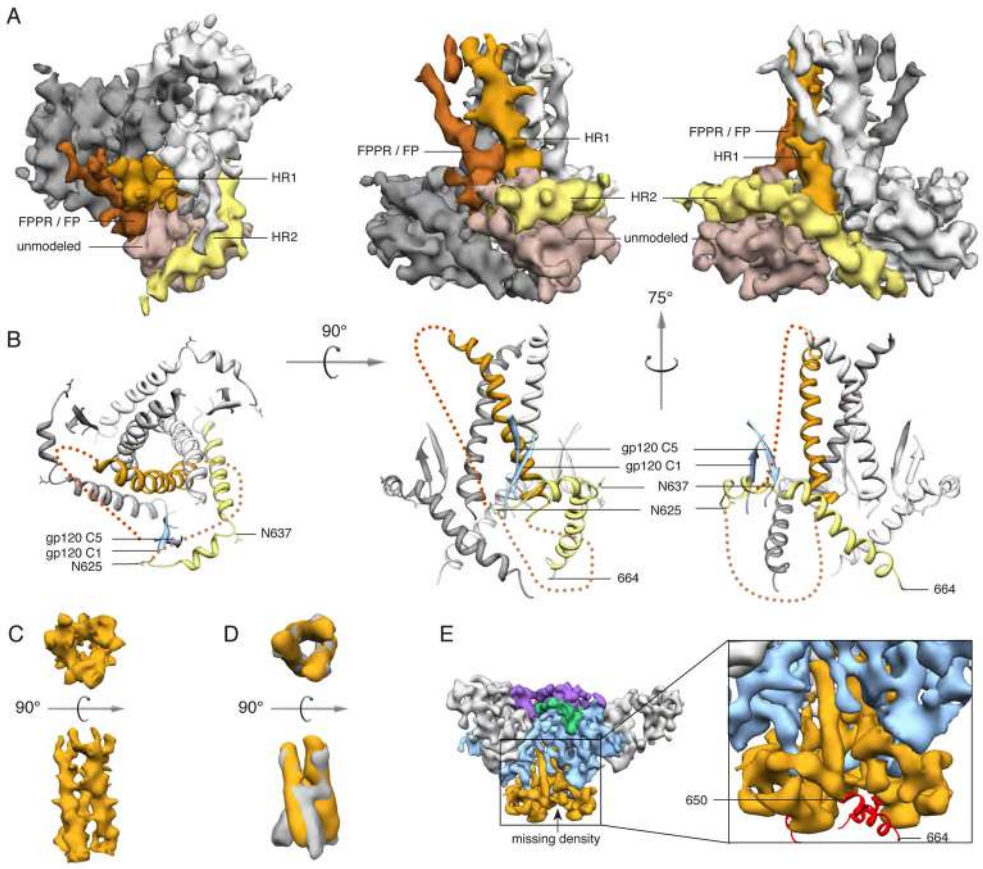

Fig. 3. Structure of gp41

(**A**) Segmented EM density map of the gp41 trimer with gp120 removed. The C-terminal half of HR1 (rust) forms a three-helix bundle at the center of the trimer, while the C-terminal half of HR2 (yellow) forms a helical structure that wraps around the trimer base. Additional density that is not assigned in the model (beige) likely corresponds to the intervening region between HR1 and HR2, including the disulfide loop, as well as C1 and C5 from gp120. Density parallel to HR1 (brown) likely corresponds to the N-terminal half of HR1, the fusion peptide proximal region (FPPR) and the fusion peptide (FP). (**B**) Modeled portion corresponding to the same views of the EM density maps in **A**. (**C**) EM density of the three-helix bundle formed by HR1 in the PGV04-bound trimer structure. (**D**) Overlay of the EM density of the three-helix bundle formed by HR1 in the PGV04-bound structure that is filtered to 9.5 Å (orange) with the 9 Å reconstruction of a 17b-bound SOSIP gp140 trimer (gray, EMDB-5462) (35). (**E**) An 8.2 Å reconstruction of a SOSIP trimer from which the last 14 amino acids were deleted (SOSIP.650:PGV04). The difference between the SOSIP.650 and SOSIP.664 maps corresponds to a short helical segment (red) at the end of HR2, that projects toward the adjacent protomer (see also fig. S8).

NIH-PA Author Manuscript

NIH-PA Author Manuscript

NIH-PA Author Manuscript

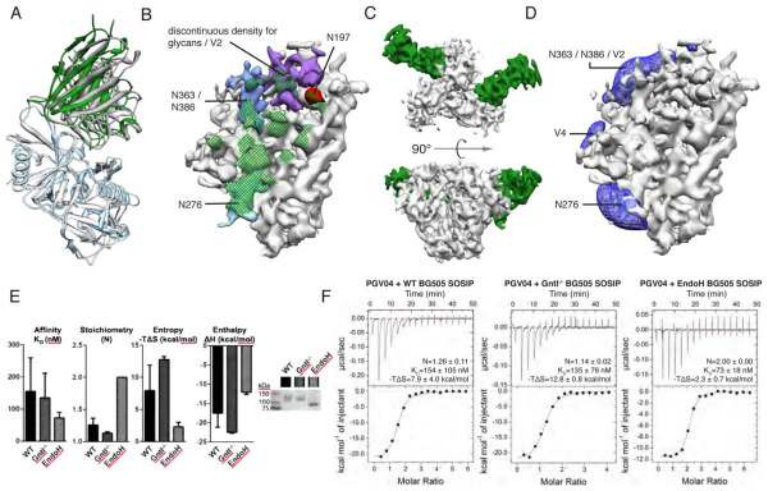

Fig. 4. PGV04 interactions with Env trimer

(**A**) Superposition of the gp120 portion of the X-ray structure of the gp120:PGV04 complex (3SE9, white/gray) and the EM structure of the SOSIP.664 trimer PGV04 complex (blue/green) illustrates subtle differences in the PGV04:gp120 interaction. Residues 121–202, 395–410 are omitted for clarity. (**B**) Elaborated nature of the CD4 binding site with densities of interest highlighted (N197 is colored red; N276 is colored light blue; N363/N386 are colored blue; V2 and/or portions of neighboring protruding glycans are colored purple). Densities corresponding to glycans and V2 are positioned to influence how the CD4bs is recognized. A glycan at N276 makes extensive interactions with the light chain of PGV04. The full PGV04 epitope on the trimer within 5 Å is denoted by green cross-hatching. (**C**) Top and side views of EM reconstruction of one BG505 SOSIP.664 trimer (white) bound to two PGV04 (green) Fabs at 7.9 Å resolution. (**D**) Difference density representing the filtered subtraction of an unliganded protomer from a PGV04-liganded protomer. Raw data is shown in fig. S16. Difference density (blue) in the vicinity of N276, N363/N383 and V2 is apparent when PGV04 is bound at the CD4bs (green). (**E**) Effect of glycosylation on PGV04 binding to the SOSIP.664 gp140 trimer, as evaluated by ITC. PGV04 binds a deglycosylated version of the same trimer with slightly higher affinity and stoichiometry, as well as reduced entropy. Bar graphs represent the mean with standard deviation for the binding affinity, stoichiometry and entropy derived from at least two independent titrations. Non-reducing SDS-PAGE shows the difference in molecular weight when the trimer is produced in 293T cells (WT) or in 293S GntI$^{-/-}$ cells before and after deglycosylation with EndoH. (**F**) Top panels show raw data and bottom panels are the binding isotherms for representative ITC binding experiments. Mean values for stoichiometry (N), binding affinity (K_D) and entropy ($-T\Delta S$), and standard deviations, calculated from at least two independent measurements.

NIH-PA Author Manuscript

NIH-PA Author Manuscript

NIH-PA Author Manuscript

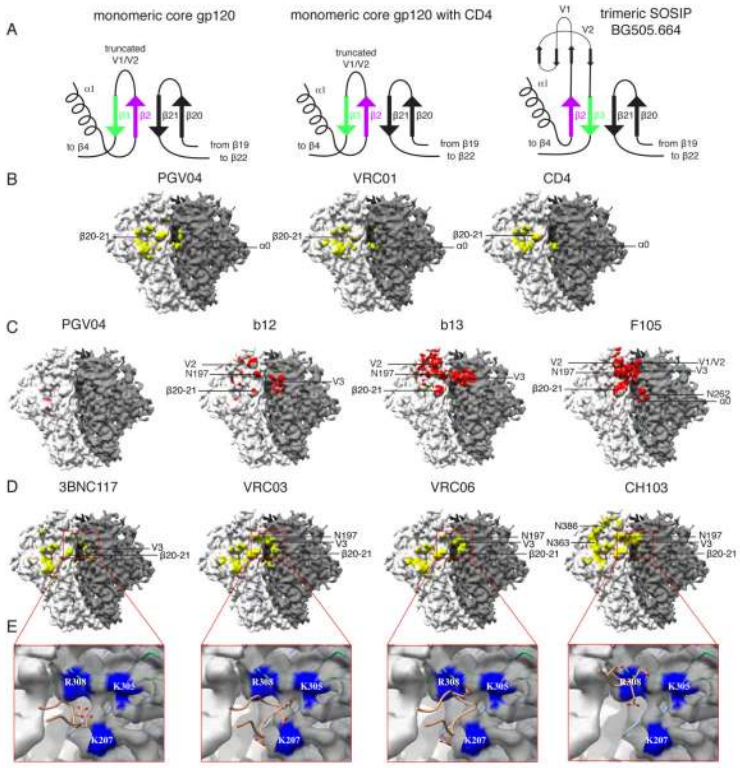

Fig. 5. Quaternary nature of the CD4 binding site

(**A**) The bridging sheet has a different topology in the trimer compared to gp120 monomer structures (e.g. PDB 1GC1, 3TGT), as illustrated by the cartoon models. Trimer formation alters how the base of V2 (β2–3) and β20–21 is arranged relative to the CD4bs (see also fig. S18). (**B**) In the EM reconstruction, the adjacent protomer appears to form additional contacts with CD4 and CD4bs bnAbs. The gp120/CD4bs Fab X-ray structures were docked into the EM map using the gp120 portion of the structure. All regions of the EM map within 5 Å of PGV04, VRC01 and CD4 have been colored yellow (fig. S20 shows all areas within 2 Å). (**C**) Major clashes with some CD4bs antibodies differ dramatically in the trimeric context. Areas of the EM map within 2 Å of the Fabs have been colored red (fig. S20 shows all areas within 5 Å). The minimal clashes with PGV04 serve as a comparator. b12 has only a few clashes with V1/V2, glycans, and V3 from the adjacent protomer, while b13 and F105 have extensive clashes. We note that, although b12 is typically a bnAb it does not neutralize the BG505 virus or bind the BG505 SOSIP.664 trimer (19). Thus, the clashes that we visualize here are consistent with each antibody being unable to neutralize the corresponding virus (19). (**D**) Areas in the EM map within 5 Å of docked Fabs, all of which contain acidic HFR3 insertions, are colored yellow (fig. S20 shows all areas within 2 Å). In addition to their previously known CD4bs epitopes, these bnAbs also interact with the V3 tip and proximal region near the protomer interface (red box). (**E**) bnAbs from **D** contain acidic HFR3 residues/insertions that interact with the basic residues in the highlighted area. Close up views of the antibody HFR3 interactions with basic residues in the trimer highlighted in the red boxed regions in **D**. Acidic residues in the HFR3 are displayed as sticks while regions in the EM map within 3 Å of basic residues have been colored blue and labeled accordingly.